Finite Volume Solution of 2D and 3D Euler and Navier-Stokes Equations

J. Fürst, M. Janda, and K. Kozel

Abstract. This contribution deals with the modern finite volume schemes solving the Euler and Navier-Stokes equations for transonic flow problems. We will mention the TVD theory for first order and higher order schemes and some numerical examples obtained by 2D central and upwind schemes for 2D transonic flows in the GAMM channel or through the SE 1050 turbine cascade of Škoda Plzeň.

In the next part two new 2D finite volume schemes are presented. Explicit composite scheme on a structured triangular mesh and implicit scheme realized on a general unstructured mesh. Both schemes are used for the solution of inviscid transonic flows in the GAMM channel and the implicit scheme also for the flows through the SE 1050 turbine cascade using both triangular and quadrilateral meshes. For the case of the flows through the SE 1050 turbine we compare the numerical results with the experiment.

The TVD MacCormack method as well as a finite volume composite scheme are extended to a 3D method for solving flows through channels and turbine cascades.

1. Mathematical model

We consider the system of 2D Navier-Stokes equations for compressible medium in conservative form:

$$\begin{array}{ll} W_t + F_x + G_y = R_x + S_y, & \\ W = [\rho, \rho u, \rho v, e], & p = (\gamma - 1)\left(e - \frac{1}{2}\rho(u^2 + v^2)\right), \\ F = [\rho u, \rho u^2 + p, \rho uv, (e+p)u], & G = [\rho v, \rho uv, \rho v^2 + p, (e+p)v], \\ R = [0, \tau_{11}, \tau_{12}, u\tau_{11} + v\tau_{12} + kT_x], & S = [0, \tau_{21}, \tau_{22}, u\tau_{21} + v\tau_{22} + kT_y], \end{array} \tag{1}$$

where ρ is the density, (u, v) the velocity vector, e the total energy per unit volume, μ the viscosity coefficient, k is the heat conductivity, p is the pressure, γ is the adiabatic coefficient, and the components of the stress tensor τ are

$$\tau_{11} = \mu\left(\frac{4}{3}u_x - \frac{2}{3}v_y\right), \quad \tau_{21} = \tau_{12} = \mu\left(u_y + v_x\right), \quad \tau_{22} = \mu\left(-\frac{2}{3}u_x + \frac{4}{3}v_y\right). \tag{2}$$

The 2D Euler equations are obtained from the Navier-Stokes equations by setting $\mu = k = 0$.

The system of 3D Euler equations is written also in conservative form (here w is the third component of the velocity vector):

$$\begin{array}{ll} W_t + F_x + G_y + H_z = 0, & W = [\rho, \rho u, \rho v, \rho w, e], \\ p = (\gamma - 1)\left(e - \frac{1}{2}\rho(u^2 + v^2 + w^2)\right), & F = [\rho u, \rho u^2 + p, \rho uv, \rho uw, (e + p)u], \\ G = [\rho v, \rho uv, \rho v^2 + p, \rho vw, (e + p)v], & H = [\rho w, \rho uw, \rho vw, \rho w^2 + p, (e + p)w]. \end{array} \tag{3}$$

The system of Euler equations is a set of first order PDE of hyperbolic type whereas the system of Navier-Stokes equations is a set of second order PDE of parabolic type.

1.1. Boundary conditions

We assume four types of boundary conditions for the case of Euler equations:

Inlet:: At the inlet we prescribe the direction of the velocity (by the inlet angle for the 2D case and by 2 angles for the 3D case), the value of the stagnation density ρ_0 and the stagnation pressure p_0. We extrapolate the static pressure p from inside and compute the other required quantities using the following relations between the stagnation and the static quantities:

$$p_0 = p\left(1 + \frac{\gamma - 1}{2}M^2\right)^{\frac{\gamma}{\gamma-1}} \qquad \rho_0 = \rho\left(1 + \frac{\gamma - 1}{2}M^2\right)^{\frac{1}{\gamma-1}}$$

where M is the local Mach number defined by $M = \sqrt{u^2 + v^2 + w^2}/a$ where the local speed of sound is $a = \sqrt{\gamma p/\rho}$. For the Navier-Stokes equations we assume $\partial T/\partial \vec{n} = 0$ and W_∞ given.

Outlet:: At the outlet we prescribe the value of the static pressure p and extrapolate the values of the density ρ and of the velocity vector from the flow field. For the viscous flows we assume again $\partial T/\partial \vec{n} = 0$.

Solid wall:: Here we prescribe the non-permeability condition ($\vec{u} \cdot \vec{n} = 0$) for the inviscid case or $\vec{u} = 0$ for the case of viscous flows. Here we assume also the adiabatic walls (i.e. $\partial T/\partial \vec{n} = 0$ where T is the temperature).

Periodicity:: Here we prescribe the periodical condition for all components of the vector of unknowns W.

2. Numerical methods

2.1. TVD schemes for one-dimensional scalar case

The theory for full nonlinear systems is very complicated and we restrict the analysis of the numerical method only to the scalar case. We assume the initial value problem for the one-dimensional scalar equation

$$u_t + f(u)_x = 0 \tag{4}$$

with the initial condition $u(x, 0) = u_0(x)$. This initial value problem is solved for $(x, t) \in R \times R_+$.

However the theoretical results are not straightforward applicable to nonlinear systems and to bounded domains, the simple model case is still important for understanding some properties of the numerical methods and as a hint for constructing good numerical methods for systems.

We approximate the weak solution to (4) by a piecewise constant function $U(x,t) = u_i^n$ for $(i-1)\Delta x < x \leq i\Delta x$ and $(n-1)\Delta t < t \leq n\Delta t$ where Δx and Δt are the mesh spacings in the space and time variables. The initial condition u^0 is computed as

$$u_i^0 = \frac{1}{\Delta x} \int_{(i-1)\Delta x}^{i\Delta x} u_0(x)\, dx. \tag{5}$$

The values u_i^n are computed for $n > 0$ using the following explicit numerical scheme written in so the called conservation form:

$$u_i^{n+1} = u_i^n - \frac{\Delta t}{\Delta x}\left[\tilde{f}(u_{i-p}^n, u_{i-p+1}^n, ..., u_{i+q}^n) - \tilde{f}(u_{i-p-1}^n, u_{i-p}^n, ..., u_{i+q-1}^n)\right] \tag{6}$$

where $\tilde{f}$ is a continuous function of $p+q+1$ parameters called the numerical flux function which approximates the physical flux function f in the following sense:

$$\forall v :: \tilde{f}(v, v, ..., v) = f(v). \tag{7}$$

The analysis of the above mentioned method is complicated even in the one-dimensional scalar case because of the nonlinearity of the flux function f (and consequently $\tilde{f}$). Nevertheless, there exist good theoretical backgrounds for certain subclasses of the general method. Namely, the following facts have been proved:

- the convergence towards the unique (so called viscosity vanishing[1]) weak solution of (4) for the class of *monotone methods*,
- the convergence towards the unique weak solution (4) for the class of *weakly TV bounded methods* (see [3] for details),
- the convergence towards the set of all weak solutions [2] of (4) for the class of *TVD methods* (see [15], [13]).

However the theory of the monotone methods is very strong and is easily extensible to the multidimensional case, the monotone methods are at most of the first order of accuracy. Therefore we prefer the class of TVD methods which is defined as follows:

Definition 2.1. *The numerical method (6) is called* total variation diminishing *(or simply* TVD*), if and only if for each numerical approximation U*

$$TV(u^{n+1}) \leq TV(u^n) = \sum_{i=-\infty}^{+\infty} |u_{i+1}^n - u_i^n|. \tag{8}$$

[1]The viscosity vanishing solution is obtained as a limit of solutions to the problems given by the equation $u_t^\epsilon + f(u^\epsilon)_x = \epsilon u_{xx}^\epsilon$ for $\epsilon \to 0+$.

[2]The uniqueness of the solution follows from Coquel's-LeFloch's theorem for the weakly TV bounded methods.

Let us consider a general one-dimensional method of the form

$$u_i^{n+1} = u_i^n - C_{i-\frac{1}{2}}(u_i^n - u_{i-1}^n) + D_{i+\frac{1}{2}}(u_{i+1}^n - u_i^n), \tag{9}$$

then the following theorem of Harten [15] can be used to check the TVD property.

Lemma 2.2 (Harten,1983)**.** *Let the following conditions be fulfilled* $\forall i \in \mathbf{Z}$*:*

$$C_{i-\frac{1}{2}} \geq 0, \qquad D_{i+\frac{1}{2}} \geq 0, \qquad C_{i+\frac{1}{2}} + D_{i+\frac{1}{2}} \leq 1. \tag{10}$$

Then the numerical method (9) is TVD.

This lemma gives some hints how to correct some classical high order methods in order to be TVD. Unfortunately, this lemma is valid only for the one-dimensional case. In fact, Goodman and LeVeque show in [12], that the TVD property in the multidimensional case implies only a first order accuracy.

In spite of their result, many methods based on one-dimensional high order TVD methods have been constructed for practical multidimensional problems. Although they are not TVD, they remain high order for smooth solutions and usually do not generate oscillations near discontinuities.

For practical computations we use the MacCormack predictor-corrector scheme because of its simple implementation especially for nonlinear systems. The TVD MacCormack scheme has for one-dimensional scalar problem the following form:

$$u_i^{n+\frac{1}{2}} = u_i^n - \frac{\Delta t}{\Delta x}\left(f(u_i^n) - f(u_{i-1}^n)\right), \tag{11}$$

$$\overline{u_i^{n+1}} = \frac{1}{2}\left[u_i^n + u_i^{n+\frac{1}{2}} - \frac{\Delta t}{\Delta x}\left(f(u_{i+1}^{n+\frac{1}{2}}) - f(u_i^{n+\frac{1}{2}})\right)\right], \tag{12}$$

$$u_i^{n+1} = \overline{u_i^{n+1}} + \left[G^+(r_i^+) + G^-(r_{i+1}^-)\right](u_{i+1}^n - u_i^n) - \left[G^+(r_{i-1}^+) + G^-(r_i^-)\right](u_i^n - u_{i-1}^n) \tag{13}$$

with $G^{\pm}$ defined by

$$G^{\pm}(r_i^{\pm}) = \frac{|f'(u_i^n)|\Delta t}{2\Delta x}\left(1 - \frac{|f'(u_i^n)|\Delta t}{\Delta x}\right)\left[1 - \Phi(r_i^{\pm})\right] \tag{14}$$

and

$$\Phi(r_i^{\pm}) = \max\left(0, \min(2r_i^{\pm}, 1)\right). \tag{15}$$

2.2. Extension to the 2D scalar case

The scalar initial value problem for the 2D problem is given by the equation $u_t + f(u)_x + g(u)_y = 0$ with the initial condition $u(x, y, 0) = u_0(x, y)$. We again solve this problem in the unbounded domain $(x, y, t) \in R \times R \times R_+$.

For a two-dimensional scalar case we analyzed in [9] a class of monotone schemes (especially the so called l^1-contractive schemes) and published in [11] the following lemma:

Lemma 2.3. *Let there exist functions* $\tilde{f}_k$ *of* $2(p+q+1)$ *parameters such that*

$$\tilde{f}(u^n_{i-p},...,u^n_{i+q}) - \tilde{f}(v^n_{i-p},...,v^n_{i+q}) = \\ = \sum_{k=-p}^{q} \tilde{f}_k(u^n_{i-p},...,u^n_{i+q},v^n_{i-p},...,v^n_{i+q})(u^n_{i+k} - v^n_{i+k}) \tag{16}$$

for arbitrary u *and* v*. If the functions* $\tilde{f}_k$ *satisfy the conditions*

$$\tilde{f}_0(u^n_{i-p},...,u^n_{i+q},v^n_{i-p},...,v^n_{i+q}) - \tilde{f}_1(u^n_{i-p-1},...,u^n_{i+q-1},v^n_{i-p-1},...,v^n_{i+q-1}) \le \frac{\Delta x}{\Delta t} \tag{17}$$

and for each $k \neq 0$ *(we set* $\tilde{f}_k = 0$ *for* $k < -p$ *and* $k > q$*) the relations*

$$\tilde{f}_k(u^n_{i-p},...,u^n_{i+q},v^n_{i-p},...,v^n_{i+q}) \le \tilde{f}_{k+1}(u^n_{i-p-1},...,u^n_{i+q-1},v^n_{i-p-1},...,v^n_{i+q-1}) \tag{18}$$

are valid, then the scheme (6) is monotone (and hence TVD).

This lemma (as well as its multidimensional variant) is proved for example in [9].

A similar lemma is valid also for multidimensional problems. Let us consider only the two-dimensional case. The total variation is defined in the this case by:

$$TV(u^n) = \Delta y \sum_{i,j} |u^n_{i+1,j} - u^n_{i,j}| + \Delta x \sum_{i,j} |u^n_{i,j+1} - u^n_{i,j}|. \tag{19}$$

Let the mesh steps be the same for both coordinates i.e. $\Delta x = \Delta y$. The weak solution is approximated by a piecewise constant function $U(x,y,t) = u^n_{i,j}$ for $(i-1)\Delta x < x \le i\Delta x$, $(j-1)\Delta y < y \le j\Delta y$, and $(n-1)\Delta t < t \le n\Delta t$. The functions $\tilde{f}_k$ and $\tilde{g}_k$ depend in a similar way as in the one-dimensional problem on $2(p+q+1)$ parameters $u^n_{i-p,j},...,u^n_{i+q,j}$, $v^n_{i-p,j},...,v^n_{i+q,j}$ for $\tilde{f}_k$ and $u^n_{i,j-p},...,u^n_{i,j+q},v^n_{i,j-p},...,v^n_{i,j+q}$ for $\tilde{g}_k$.

Lemma 2.4. *Let there exist functions* $\tilde{f}_k$ *and* $\tilde{g}_k$ *of* $2(p+q+1)$ *parameters such that*

$$\tilde{f}(u^n_{i-p,j},...,u^n_{i+q,j}) - \tilde{f}(v^n_{i-p,j},...,v^n_{i+q,j}) = \sum_{k=-p}^{q} \tilde{f}_k(u^n_{i-p,j},...,v^n_{i+q,j})(u^n_{i+k,j} - v^n_{i+k,j}) \tag{20}$$

$$\tilde{g}(u^n_{i,j-p},...,u^n_{i,j+q}) - \tilde{g}(v^n_{i,j-p,},...,v^n_{i,j+q}) = \sum_{k=-p}^{q} \tilde{g}_k(u^n_{i,j-p},...,v^n_{i,j+q})(u^n_{i,j+k} - v^n_{i,j+k}) \tag{21}$$

for each arbitrary u *and* v*. If the functions* $\tilde{f}_k$ *and* $\tilde{g}_k$ *satisfy the conditions*

$$\begin{aligned} \tilde{f}_0(u^n_{i-p,j},...,v^n_{i+q,j}) &- \tilde{f}_1(u^n_{i-p-1,j},...,v^n_{i+q-1,j}) + \\ \tilde{g}_0(u^n_{i,j-p},...,v^n_{i,j+q}) &- \tilde{g}_1(u^n_{i,j-p-1},...,v^n_{i,j+q-1}) \le \frac{\Delta x}{\Delta t} \end{aligned} \tag{22}$$

and for each $k \neq 0$ (we set $\tilde{f}_k = 0$ and $\tilde{f}_k = 0$ for $k < -p$ and $k > q$)

$$\begin{aligned} \tilde{f}_k(u^n_{i-p,j}, ..., v^n_{i+q,j}) &\leq \tilde{f}_{k+1}(u^n_{i-p-1,j}, ..., v^n_{i+q-1,j}), \quad (23) \\ \tilde{g}_k(u^n_{i,j-p}, ..., v^n_{i,j+q}) &\leq \tilde{g}_{k+1}(u^n_{i,j-p-1}, ..., v^n_{i,j+q-1}) \quad (24) \end{aligned}$$

then the scheme

$$\begin{aligned} u^{n+1}_{i,j} &= u^n_{i,j} - \frac{\Delta t}{\Delta x}\left(\tilde{f}^n_{i+\frac{1}{2},j} - \tilde{f}^n_{i-\frac{1}{2},j}\right) - \frac{\Delta t}{\Delta y}\left(\tilde{g}^n_{i,j+\frac{1}{2}} - \tilde{g}^n_{i,j-\frac{1}{2}}\right), \quad (25) \\ \tilde{f}^n_{i+\frac{1}{2},j} &= \tilde{f}(u^n_{i-p,j}, u^n_{i-p+1,j}, ..., u^n_{i+q,j}), \quad \tilde{g}^n_{i,j+\frac{1}{2}} = \tilde{g}(u^n_{i,j-p}, u^n_{i,j-p+1}, ..., u^n_{i,j+q}) \end{aligned}$$

is monotone (and hence TVD).

Unfortunately it is not possible to construct a high order TVD scheme for multidimensional problem [12]. The uniform TVD bound is too restrictive and therefore one should consider following approach analyzed for example by Coquel and LeFloch in [4, 3]. Let us assume a two-dimensional conservative scheme of the form:

$$u^{n+1}_{i,j} = u^n_{i,j} - \frac{\Delta t}{\Delta x}\left(\tilde{f}^n_{i+\frac{1}{2},j} - \tilde{f}^n_{i-\frac{1}{2},j}\right) - \frac{\Delta t}{\Delta y}\left(\tilde{g}^n_{i,j+\frac{1}{2}} - \tilde{g}^n_{i,j-\frac{1}{2}}\right), \quad (26)$$

with $\Delta x = \Delta y = const.\Delta t$ and consistent with the equation $u_t + f(u)_x + g(u)_y = 0$.

Theorem 2.5 (Coquel, LeFloch 1991)**.** *Let the numerical fluxes $f^n_{i+\frac{1}{2},j}$ and $g^n_{i,j+\frac{1}{2}}$ can be split onto two parts $f^n_{i+\frac{1}{2},j} = p^n_{i+\frac{1}{2},j} + \frac{\Delta x}{\Delta t}a^n_{i+\frac{1}{2},j}$ and $g^n_{i,j+\frac{1}{2}} = q^n_{i,j+\frac{1}{2}} + \frac{\Delta y}{\Delta t}b^n_{i,j+\frac{1}{2}}$ with p and q being monotone fluxes (e.g. first order Lax-Friedrichs type) and a and b being antidiffusive high order corrections. If there exist for a finite time $T > 0$ constants $C > 0$ and $M > 0$ independent of Δt (and consequently independent of Δx and Δy) such that*

$$||u^n_{i,j}||_\infty < C, \qquad |a^n_{i+\frac{1}{2},j}| < M\Delta x^\alpha, \qquad |b^n_{i,j+\frac{1}{2}}| < M\Delta y^\alpha, \quad (27)$$

with $n\Delta t < T$ and $\alpha \in (\frac{2}{3}, 1)$, then the piecewise constant function with the values given by $u^n_{i,j}$ converges to the unique entropy solution when $\Delta t \to 0$.

Example 2.6 (2D version of the scheme proposed by Davis)**.** *Let us suppose the 2D scheme for the two-dimensional linear equation proposed by Davis $u_t + cu_x + du_y = 0$:*

$$\begin{aligned} u^{n+1}_{i,j} &= u^n_{i,j} - c\frac{\Delta t}{2\Delta x}(u^n_{i+1,j} - u^n_{i-1,j}) + c^2\frac{\Delta t^2}{2\Delta x^2}(u^n_{i+1,j} - 2u^n_{i,j} + u^n_{i-1,j}) + \\ &+ K(r^+_{i,j}, r^-_{i+1,j})(u^n_{i+1,j} - u^n_{i,j}) - K(r^+_{i-1,j}, r^-_{i,j})(u^n_{i,j} - u^n_{i-1,j}) - \quad (28) \\ &- d\frac{\Delta t}{2\Delta y}(u^n_{i,j+1} - u^n_{i,j-1}) + d^2\frac{\Delta t^2}{2\Delta y^2}(u^n_{i,j+1} - 2u^n_{i,j} + u^n_{i,j-1}) + \\ &+ K(s^+_{i,j}, s^-_{i,j+1})(u^n_{i,j+1} - u^n_{i,j}) - K(s^+_{i,j-1}, s^-_{i,j})(u^n_{i,j} - u^n_{i,j-1}) \quad (29) \end{aligned}$$

where

$$K(r^+_{i,j}, r^-_{i+1,j}) = \frac{|c|\Delta t}{2\Delta x}(1 - \frac{|c|\Delta t}{\Delta x}) \left[1 - \tilde{\Phi}(r^+_{i,j}, r^-_{i+1,j})\right] \quad (30)$$

$$K(s^+_{i,j}, s^-_{i,j+1}) = \frac{|c|\Delta t}{2\Delta y}(1 - \frac{|c|\Delta t}{\Delta y}) \left[1 - \tilde{\Phi}(s^+_{i,j}, s^-_{i,j+1})\right] \quad (31)$$

$$\tilde{\Phi}(r^+_{i,j}, r^-_{i+1,j}) = \max\left(0, \min(2r^+_{i,j}, r^-_{i+1,j}, 1), \min(r^+_{i,j}, 2r^-_{i+1,j}, 1)\right) \quad (32)$$

$$\tilde{\Phi}(s^+_{i,j}, s^-_{i,j+1}) = \max\left(0, \min(2s^+_{i,j}, s^-_{i,j+1}, 1), \min(p^+_{i,j}, 2p^-_{i,j+1}, 1)\right) \quad (33)$$

$$r^+_{i,j} = (u^n_{i,j} - u^n_{i-1,j})/(u^n_{i+1,j} - u^n_{i,j}) \quad (34)$$

$$r^-_{i,j} = (u^n_{i+1,j} - u^n_{i,j})/(u^n_{i,j} - u^n_{i-1,j}) \quad (35)$$

$$s^+_{i,j} = (u^n_{i,j} - u^n_{i,j-1})/(u^n_{i,j+1} - u^n_{i,j}) \quad (36)$$

$$s^-_{i,j} = (u^n_{i,j+1} - u^n_{i,j})/(u^n_{i,j} - u^n_{i,j-1}). \quad (37)$$

Let us replace $\tilde{\Phi}$ *by the new limiter:*

$$\overline{\tilde{\Phi}}(r^+_{i,j}, r^-_{i+1,j}) = \min\left(\tilde{\Phi}(r^+_{i,j}, r^-_{i+1,j}), \frac{M'\Delta x^\alpha}{|u^n_{i+1,j} - u^n_{i,j}|}\right) \quad (38)$$

$$\overline{\tilde{\Phi}}(s^+_{i,j}, s^-_{i,j+1}) = \min\left(\tilde{\Phi}(s^+_{i,j}, s^-_{i,j+1}), \frac{M'\Delta y^\alpha}{|u^n_{i,j+1} - u^n_{i,j}|}\right). \quad (39)$$

Then the antidiffusive fluxes a and b are bounded by $M'\Delta x^\alpha$ *and* $M'\Delta y^\alpha$ *respectively and the modification of the two-dimensional scheme is convergent.*

Similar theorem is valid also for three-dimensional case.

2.3. TVD schemes for hyperbolic systems

Let us consider a linear system

$$W_t + AW_x = 0. \quad (40)$$

The solution is now a vector-valued function $W : \mathbf{R} \times \mathbf{R}^+ \to \mathbf{R}^m$ (m is the number of equations) and A is an $m \times m$ constant matrix. The system (40) is called *hyperbolic* if the matrix A has m real eigenvalues and m linearly independent right eigenvectors. In that case, we can decompose the matrix A into

$$A = R\Lambda R^{-1} \quad (41)$$

where R is the regular matrix composed of the eigenvectors of A and Λ is the diagonal matrix containing the eigenvalues of A ($\Lambda = \mathrm{diag}(a^{(1)}, ..., a^{(m)})$).

Let us define a new set of variables by $V = R^{-1}W$ (we call it the *characteristic variables*). Multiplying the original system (40) by R^{-1} one gets

$$R^{-1}W_t + R^{-1}AW_x = 0 \quad (42)$$

and hence, using the characteristic variables,

$$V_t + \Lambda V_x = 0 \quad (43)$$

which is a set of m independent scalar problems. For each component we can use the TVD MacCormack scheme defined in the previous section. In order to get the TVD MacCormack scheme for the original variables W, we multiply the scheme written for the characteristic variables V by the matrix R. Finally, we get

$$
\begin{aligned}
W_i^{n+\frac{1}{2}} &= W_i^n - \frac{\Delta t}{\Delta x}\left(AW_i^n - AW_{i-1}^n\right), && (44)\\
\overline{W_i^{n+1}} &= \frac{1}{2}\left[W_i^n + W_i^{n+\frac{1}{2}} - \frac{\Delta t}{\Delta x}\left(AW_{i+1}^{n+\frac{1}{2}} - AW_i^{n+\frac{1}{2}}\right)\right], && (45)\\
W_i^{n+1} &= \overline{W_i^{n+1}} + R\left[\tilde{G}^+(\tilde{r}_i^+) + \tilde{G}^-(\tilde{r}_{i+1}^-)\right] R^{-1}(W_{i+1}^n - W_i^n) - \\
&\quad -R\left[\tilde{G}^+(\tilde{r}_{i-1}^+) + \tilde{G}^-(\tilde{r}_i^-)\right] R^{-1}(W_i^n - W_{i-1}^n). && (46)
\end{aligned}
$$

Here $\tilde{r}_i^{\pm}$ are vectors with m components

$$
\begin{aligned}
(\tilde{r}_i^+)^{(l)} &= \left(R^{-1}(W_i^n - W_{i-1}^n)\right)^{(l)} / \left(R^{-1}(W_{i+1}^n - W_i^n)\right)^{(l)}, && (47)\\
(\tilde{r}_i^-)^{(l)} &= \left(R^{-1}(W_{i+1}^n - W_i^n)\right)^{(l)} / \left(R^{-1}(W_i^n - W_{i-1}^n)\right)^{(l)}, && (48)
\end{aligned}
$$

where $r^{(l)}$ denotes the l-th component of the vector r.

The viscosity coefficients $\tilde{G}$ are $m \times m$ diagonal matrices with the elements given by

$$
\tilde{G}^{\pm}(\tilde{r}_i^{\pm})^{(l,l)} = \frac{1}{2}\frac{|a^{(l)}|\Delta t}{\Delta x}\left(1 - \frac{|a^{(l)}|\Delta t}{\Delta x}\right)[1 - \Phi((\tilde{r}_i^{\pm})^{(l)})]. \qquad (49)
$$

In order to avoid the evaluation of eigenvectors of the Jacobian matrix A we use the so called simplified TVD scheme proposed by D. M. Causon in [2] which is for the case of the one-dimensional nonlinear system written as:

$$
\begin{aligned}
W_i^{n+\frac{1}{2}} &= W_i^n - \frac{\Delta t}{\Delta x}\left(F(W_i^n) - F(W_{i-1}^n)\right), && (50)\\
\overline{W_i^{n+1}} &= \frac{1}{2}\left[W_i^n + W_i^{n+\frac{1}{2}} - \frac{\Delta t}{\Delta x}\left(F(W_{i+1}^{n+\frac{1}{2}}) - F(W_i^{n+\frac{1}{2}})\right)\right], && (51)\\
W_i^{n+1} &= \overline{W_i^{n+1}} + \left[\overline{G}^+(\overline{r}_i^+) + \overline{G}^-(\overline{r}_{i+1}^-)\right](W_{i+1}^n - W_i^n) - \\
&\quad - \left[\overline{G}^+(\overline{r}_{i-1}^+) + \overline{G}^-(\overline{r}_i^-)\right](W_i^n - W_{i-1}^n) && (52)
\end{aligned}
$$

with $\overline{G}^{\pm}$ and $\overline{r}^{\pm}$ given by the formulas

$$
\begin{aligned}
\overline{r}_i^+ &= \frac{<W_i^n - W_{i-1}^n, W_{i+1}^n - W_i^n>}{<W_{i+1}^n - W_i^n, W_{i+1}^n - W_i^n>}, \qquad \overline{r}_i^- = \frac{<W_i^n - W_{i-1}^n, W_{i+1}^n - W_i^n>}{<W_i^n - W_{i-1}^n, W_i^n - W_{i-1}^n>},\\
\overline{G}^{\pm}(\overline{r}_i^{\pm}) &= \tfrac{1}{2}C(\nu_i)\left[1 - \Phi(\overline{r}_i^{\pm})\right], \qquad C(\nu_i) = \begin{cases} \nu_i(1-\nu_i), & \nu_i \le 0.5 \\ 0.25, & \nu_i > 0.5, \end{cases}\\
\nu_i &= \rho_{A_i}\tfrac{\Delta t}{\Delta x}.
\end{aligned} \qquad (53)
$$

Here $<.,.>$ denotes the standard inner (scalar) product in $\mathbf{R}^m$ and ρ_{A_i} is the spectral radius of the Jacobi matrix $\partial F/\partial W$ at the point W_i (for the case of the

Euler equations, $\rho_{A_i} = |u_i| + c_i$ where u_i is the local flow speed and c_i is the local sound speed.

3. Composite schemes

In the simplest 1D case there exist two forms of Lax-Friedrichs (LF) scheme:

1. standard one-step version (non-staggered scheme):

$$W_i^{n+1} = \frac{1}{2}(W_{i+1}^n + W_{i-1}^n) - \frac{\Delta t}{2\Delta x}(F_{i+1}^n - F_{i-1}^n), \tag{54}$$

2. two-step version (staggered scheme):

$$W_{i+1/2}^* = \frac{1}{2}(W_{i+1}^n + W_i^n) - \frac{\Delta t}{2\Delta x}(F_{i+1}^n - F_i^n), \tag{55}$$

$$W_i^{n+1} = \frac{1}{2}(W_{i+1/2}^* + W_{i-1/2}^*) - \frac{\Delta t}{2\Delta x}(F_{i+1/2}^* - F_{i-1/2}^*). \tag{56}$$

The two-step Lax-Wendroff (LW) scheme can be written as:

1. non-staggered scheme:

$$W_i^* = W_i^n - \frac{\Delta t}{4\Delta x}(F_{i+1}^n - F_{i-1}^n) + \epsilon(W_{i+1}^n - 2W_i^n + W_{i-1}^n), \tag{57}$$

$$W_i^{n+1} = W_i^n - \frac{\Delta t}{2\Delta x}(F_{i+1}^* - F_{i-1}^*), \tag{58}$$

2. or staggered scheme:

$$W_{i+1/2}^* = \frac{1}{2}(W_{i+1}^n + W_i^n) - \frac{\Delta t}{2\Delta x}(F_{i+1}^n - F_i^n), \tag{59}$$

$$W_i^{n+1} = W_{i+1}^n - \frac{\Delta t}{\Delta x}(F_{i+1/2}^* - F_{i-1/2}^*). \tag{60}$$

The one-dimensional composite scheme LWLFN is given by (N-1) LW steps followed by one LF step:

$$W^{n+N} = LF \circ \underbrace{LW \circ LW \circ ... \circ LW}_{N-1} W^n. \tag{61}$$

The extension for two-dimensional case is done using the finite volume approach. Let us assume a triangular mesh with triangles denoted by T_i. The cell-centered LF scheme corresponding to the one-dimensional LF non-staggered scheme is given by:

$$W_i^{n+1} = \frac{1}{3}\sum_{k=1}^{3} W_k^n - \frac{\Delta t}{\mu_i}\sum_{k=1}^{3}(F_{k,i}^n \Delta y_k - G_{k,i}^n \Delta x_k) \tag{62}$$

where $\mu_i = \int\int_{T_i} dx\, dy$, $F_{k,i}^n = (F_k^n + F_i^n)/2$, $G_{k,i}^n = (G_k^n + G_i^n)/2$ and W_k^n is the value of W at the one of three neighboring triangles T_k of the triangle T_i.

For the two-step LW scheme one has:

$$W_i^{n+1/2} = \frac{1}{3}\sum_{k=1}^{3} W_k^n - \frac{\Delta t}{2\mu_i}\sum_{k=1}^{3}(F_{k,i}^n \Delta y_k - G_{k,i}^n \Delta x_k), \tag{63}$$

$$W_i^{n+1} = W_i^n - \frac{\Delta t}{\mu_i}\sum_{k=1}^{3}(F_{k,i}^{n+1/2} \Delta y_k - G_{k,i}^{n+1/2} \Delta x_k). \tag{64}$$

The cell-vertex corresponding to the one-dimensional staggered version has the following form (assuming for simplicity that six triangles meet at each vertex): LF:

$$W_i^* = \frac{1}{3}\sum_{k=1}^{3} W_{0,k}^n - \frac{\Delta t}{2\mu_i}\sum_{k=1}^{3}(\tilde{F}_k \Delta y_k - \tilde{G}_k \Delta x_k), \tag{65}$$

$$\tilde{F}_k = \frac{1}{2}(F_{0,k+1} - F_{0,k}),\ \tilde{G}_k = \frac{1}{2}(G_{0,k+1} - G_{0,k}),$$

$$W_{0,k}^{n+1} = \frac{1}{6}\sum_{i=1}^{6} W_i^* - \frac{\Delta t}{2\mu_{0,k}}\sum_{i=1}^{6}(\tilde{F}_i^* \Delta y_i - \tilde{G}_i^* \Delta x_y), \tag{66}$$

$$\tilde{F}_i^* = \frac{1}{2}(F_{i+1}^* - F_i^*),\ \tilde{G}_i^* = \frac{1}{2}(G_{i+1}^* - G_i^*).$$

LW scheme uses the same first step as the above described LF scheme and the second step is of the form:

$$W_{0,k}^{n+1} = W_{0,k}^n - \frac{\Delta t}{2\mu_{0,k}}\sum_{i=1}^{6}(\tilde{F}_i^* \Delta y_i - \tilde{G}_i^* \Delta x_y). \tag{67}$$

Here $W_{0,k}$ are located at the vertices $V_{0,k}$ of the triangle T_i and W_i^* are located at the centers of gravity P_i of triangles T_i.

The composite scheme consists again as $N-1$ steps of LW scheme followed by one LF step. The value of N is determined by numerical testing. The cell vertex scheme was also extended to three-dimensional case.

Remark: Composite schemes were introduced by R. Liska and B. Wendroff for a 2D nonlinear hyperbolic problem solved by finite difference methods on an orthogonal grid. The idea is following: in many high order schemes one has to add some artificial viscosity terms in order to achieve solution without oscillations near shock waves or steep gradients. Composite schemes use certain number of a high order scheme (with low value of artificial viscosity) and the arising oscillations are then smeared by one step of a more dissipative scheme (for example Lax-Friedrichs scheme).

We extended the original finite difference schemes to 2D and 3D finite volume method of the cell centered or cell vertex form [14].

4. Implicit finite volume method for 2D inviscid flows

The numerical solution is again obtained by the finite volume approach: The domain Ω is approximated by a polygonal domain Ω_h and this polygonal domain is divided into m polygonal convex cells[3] C_i possess the following property:

$$\overline{\Omega_h} = \bigcup_{i=1}^{m} \overline{C_i} \text{ and } C_i \cap C_j = \emptyset \text{ for } i \neq j \ .$$

Figure 1 shows a sample of such a domain divided into 13 triangular, quadrilateral, and pentagonal cells. Let m_i denote the number of cells adjacent to C_i (i.e. number of cells that share an edge with the cell C_i) and let the set $N_i = \{i_1, i_2, ..., i_{m_i}\}$ contain their indices (see Fig. 1 where $m_i = 5$). Next, let us denote by B_i^{inlet} the set of edges shared by the cell C_i and the inlet boundary Γ_h^{inlet} of Ω_h; similarly for B_i^{outlet} and B_i^{wall}.

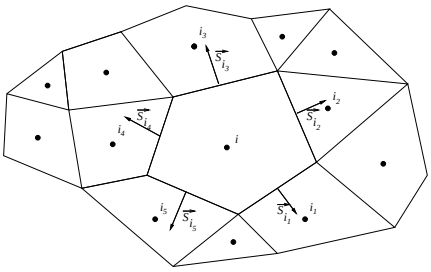

FIGURE 1. Unstructured grid with mixed type of cells.

The basic finite volume scheme is obtained in the usual way: integrating the conservation law in a cell C_i, applying Green's theorem and approximating the integral over the boundary of C_i by the numerical flux functions. The scheme is then

$$W_i^{n+1} = W_i^n - \Delta t R^1(W^n)_i. \tag{68}$$

Here W_i^n stands for the approximation of the solution in the cell C_i at a time $t = n\Delta t$ and $R^1(W^n)_i$ is the component of the residual vector computed as

$$R^1(W^n)_i = \frac{1}{\mu(C_i)} \left[\sum_{j \in N_i} H(W_i^n, W_j^n, \vec{S}_{i,j}) + \sum_b \sum_{e \in B_i^b} H^b(W_i^n, \vec{S}_e) \right]. \tag{69}$$

The superscript 1 denotes the first order approximation, $\mu(C_i)$ is the volume of the cell C_i, $\vec{S}_{i,j}$ denotes the outer normal vector to the common edge between C_i and C_j, the function H is the numerical flux, b denotes the type of the boundary conditions and belongs to the set $b \in \{inlet, outlet, wall\}$, H^b is the numerical flux through the boundary and $\vec{S}_e$ denotes the outer normal vector to the boundary edge e. Both vectors $\vec{S}_{i,j}$ and $\vec{S}_e$ have the length equal to the length of the corresponding edge. The numerical flux $H(W_i^n, W_j^n, \vec{S}_{i,j})$ in the previous formula is the numerical approximation of the integral of the physical flux function over the

[3]Since the structured grid can be viewed from the mathematical point of view as a special case of the unstructured grid, we present only the scheme for unstructured meshes.

common edge $e_{i,j}$ shared between C_i and C_j:

$$H(W_i^n, W_j^n, \vec{S}_{i,j}) \approx \int_{e_{i,j}} \left(\begin{pmatrix} \rho u \\ \rho u^2 + p \\ \rho uv \\ (e+p)u \end{pmatrix} n_x + \begin{pmatrix} \rho v \\ \rho uv \\ \rho v^2 + p \\ (e+p)v \end{pmatrix} n_y \right) dS \qquad (70)$$

where n_x and n_y are the components of the unit normal vector to the edge $e_{i,j}$ oriented as the outer normal for the cell C_i. Analogous, $H^b(W_i^n, \vec{S}_e)$ is the approximation of the flux through the edge on the boundary.

4.1. First order implicit scheme

As a building block for the implicit scheme we choose the first order finite volume scheme based on Osher's flux and the related approximate Riemann solver (see [16]). The advantage of the Osher flux is that one can evaluate simply the Jacobians of the numerical flux function which are needed for the implicit scheme.

The usual explicit first order scheme is then

$$W^{n+1} = W^n - \Delta t R^1(W^n) \qquad (71)$$

and the implicit scheme is obtained from the explicit version (68) by replacing $R^1(W^n)$ by $R^1(W^{n+1})$:

$$W_i^{n+1} = W_i^n - \Delta t R^1(W^{n+1})_i. \qquad (72)$$

The operator R is nonlinear, so we can't solve this equation directly. Therefore we linearize the equation at the point W^n:

$$W^{n+1} = W^n - \Delta t \left(R^1(W^n) + \frac{\partial R^1}{\partial W} \left(W^{n+1} - W^n \right) \right), \qquad (73)$$

hence,

$$\left(\frac{\mathbf{I}}{\Delta t} + \frac{\partial R^1}{\partial W} \right) \left(W^{n+1} - W^n \right) = -R^1(W^n). \qquad (74)$$

The matrix $\frac{\partial R^1}{\partial W}$ is evaluated at the point W^n using the expressions for the Jacobian matrices of Osher's flux functions $\frac{\partial H(W_L, W_R, \vec{S})}{\partial W_L}$ and $\frac{\partial H(W_L, W_R, \vec{S})}{\partial W_R}$ and the appropriate Jacobian matrices of boundary fluxes.

The resulting system of linearized equations is solved using a GMRES method preconditioned with the ILU decomposition.

4.2. Second order semi-implicit scheme

In order to improve the accuracy of the basic first order scheme we use a piecewise linear reconstruction of the solution (for details see [10]). The second order semi-implicit scheme uses the high order residual R^2 on the right hand side (explicit part) and the matrix on the left hand side is computed from the low order residual:

$$\left(\frac{\mathbf{I}}{\Delta t} + \frac{\partial R^1}{\partial W} \right) \left(W^{n+1} - W^n \right) = -R^2(W^n). \qquad (75)$$

The second order residual R^2 is computed in the following way: we compute first the approximation of the gradient of the solution $\overline{\text{grad}}W^n$ in each cell [4] and then using this gradient we define the second order residual vector by

$$\begin{aligned} W^L_{i,j} &= W^n_i + (\vec{x}_{i,j} - \vec{x}_i) \cdot \overline{\text{grad}}W^n_i, \\ W^R_{i,j} &= W^n_j + (\vec{x}_{j,i} - \vec{x}_j) \cdot \overline{\text{grad}}W^n_j, \\ R^2(W^n)_i &= \frac{1}{\mu(C_i)} \left[\sum_{j \in N_i} H(W^L_{i,j}, W^R_{i,j}, \vec{S}_{i,j}) + \sum_b \sum_{e \in B^b_i} H^b(W^L_{i,j}, \vec{S}_e) \right], \end{aligned} \tag{76}$$

where $\vec{x}_i$ is the center of gravity of the cell i and $\vec{x}_{i,j}$ is the center of the common edge between the cells i and j. The numerical fluxes H and H^b are computed in the same way as for the first order scheme (i.e. using Osher's Riemann solver) but instead of W_i and W_j we use the interpolated values $W^R_{i,j}$ and $W^L_{i,j}$.

In the steady case one has $R^2(W^n) = 0$ and therefore the scheme is high order. Moreover, as the second order residual is of ENO type, the stationary solution is essentially non-oscillatory. In the unsteady case the scheme is only low order due to replacing R^2 by R^1 in the implicit part.

5. 2D transonic inviscid flow through a channel and a turbine cascade

5.1. Transonic flow through the 2D test channel with a bump

As a first test case we choose the transonic flow through the two-dimensional test channel with a bump, i.e. the so-called Ron-Ho-Ni channel. This is a well-known test case and it was solved by many researchers. See for example [5], [6].

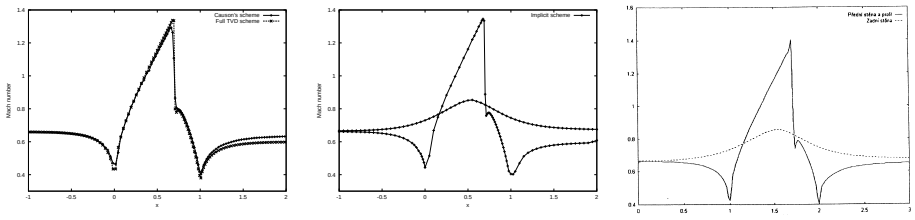

(a) TVD MacCormack scheme

(b) Implicit scheme

(c) Composite scheme

FIGURE 2. Distribution of the Mach number along the lower and upper walls for the 2D channel.

[4] The evaluation of the gradients is described in in detail [10].

We use the structured mesh with 120×30 quadrilateral cells for the TVD MacCormack scheme, an unstructured triangular mesh with 4424 triangles (with refinement in the vicinity of the shock wave) for the implicit scheme and a structured triangular mesh with 10800 triangles for the composite scheme. At the inlet ($x = -1$) we prescribe the stagnation pressure $p_0 = 1$, the stagnation density $\rho_0 = 1$ and the inlet angle $\alpha_1 = 0$. At the outlet we keep the pressure $p_2 = 0.737$. The upper ($y = 1$) and lower part are solid walls.

Figure 2(a) shows the distribution of the Mach number along the upper and the lower wall after 30000 iterations of two above mentioned variants of the MacCormack scheme with $CFL = 0.5$ while figure 2(b) shows the results obtained by the implicit scheme and figure 2(c) by the composite scheme.

We can see that the results obtained by the full TVD MacCormack scheme are quite good. Causon's simplified scheme uses too much artificial dissipation.

5.2. Transonic flow through the 2D turbine cascade SE 1050

Next we solve the transonic flow through the 2D turbine cascade SE 1050 given by Škoda Plzeň. Figure 3 shows the results of the interferometric measurement obtained for the inlet Mach number $M_1 = 0.395$ [17]. One can see the characteristic structure of the shock waves emitted from the outlet edge and the reflected shock waves. Moreover, one can notice the recompression zone on the suction side of the blade. Our computation was performed on a structured mesh with 200×40 quadrilateral cells for the full TVD MacCormack scheme (see Fig. 4(a)) and on an unstructured mesh with 7892 triangles for the implicit scheme (Fig. 4(b)).

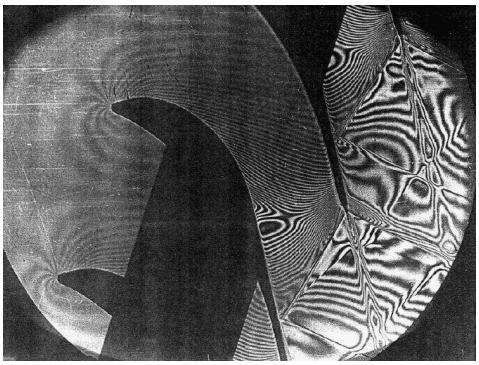

FIGURE 3. Interferometric measurement of SE 1050

5.3. Laminar viscous flow through a 2D turbine cascade

Next we solve the transonic viscous flow through the DCA 8% cascade. We consider the flow with the non-dimensional viscosity $\mu = 10^{-4}$ which gives, for the inlet conditions $p_0 = 1$, $\rho_0 = 1$, $\alpha_1 = 2^o$ and outlet pressure $p_2 = 0.48$, the value of

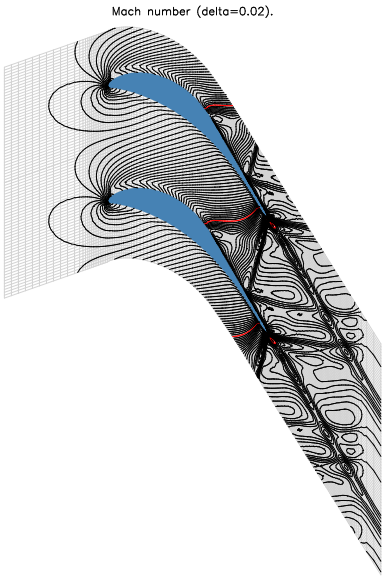

(a) TVD MacCormack scheme, structured grid

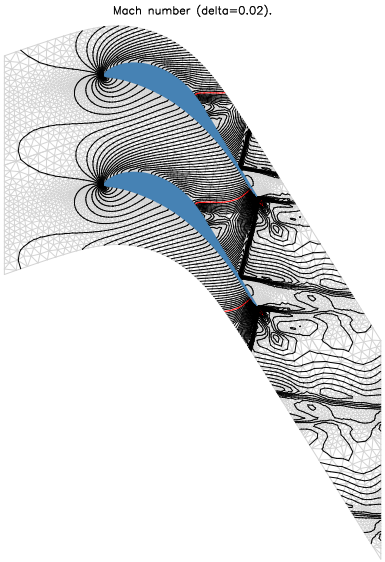

(b) Implicit scheme, unstructured grid

FIGURE 4. Distribution of the Mach number in a 2D turbine cascade

the Reynolds number $Re = 6450$, inlet Mach number $M_1 = 0.76$ and outlet Mach number $M_2 = 1.03$.

We use a simple structured mesh with 90×50 quadrilateral cells refined in the vicinity of profiles. Figure 5 shows the results obtained by an improved version of Causon's scheme [5] after 50000 and 50200 iterations. We can see that the solution is non-stationary (see the changes in the shape of the wake). Similar non-stationary solution was obtained also by using a finite difference ENO scheme [1]. Let us mention that these flow conditions (it means relatively low Reynolds number and high Mach number) are not interesting for practical applications. We have done this computation in order to show that the effects of artificial viscosity can be very important for a viscous flow calculation. As a matter of fact, a similar case was formerly solved by M. Huněk and K. Kozel [8] using an implicit residual averaging method. Their method gave stationary results whereas our computation leads to a non-stationary solution. This is probably due to the fact, that the residual smoothing method uses too much artificial viscosity.

[5] The so called modified scheme which we published for example in [11].

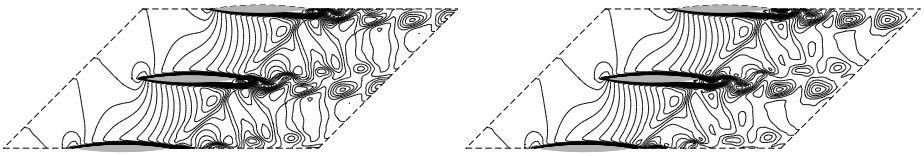

(a) 50000 time steps (b) 50200 time steps

FIGURE 5. Isolines of Mach number for the non-stationary laminar transonic flow through the DCA 8% cascade.

6. 3D inviscid transonic flows

6.1. 3D transonic flow through a channel

The 2D composite scheme of cell-vertex type was extended to 3D case using the following finite volume mesh given by fig. 6. Figure 6(a) shows basic finite volume, fig. 6(b) shows the dual finite volume and fig. 6(c) shows the global 3D basic mesh. We used $180 \times 30 \times 12$ mesh and 3D channel was changed by bump with the height

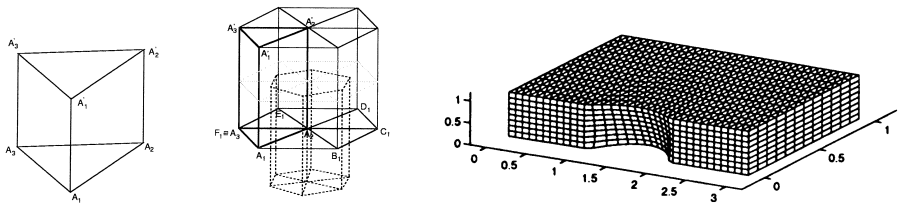

(a) Basic cell (b) Dual cell (c) Global mesh

FIGURE 6. 3D finite volume mesh for composite schemes.

equal to 0.18 at $z = 0$ decreasing to 0.10 at $z = 1$. Figure 7 shows Mach number distribution in the planes $z = const.$. Figure 7(a) shows the solution at the wall with the bump (with the shock wave) and smooth solution at the upper wall. Figure 7(b) shows the change of the strength of the shock wave for z between 0 and 1. Here we use 25 steps of LW scheme followed by 1 LF step.

6.2. 3D transonic flow through a turbine cascade

The three-dimensional Causon's scheme and its improved variant are used for the computation of the transonic flow through the stator stage of the real 3D turbine given by Škoda Plzeň company.

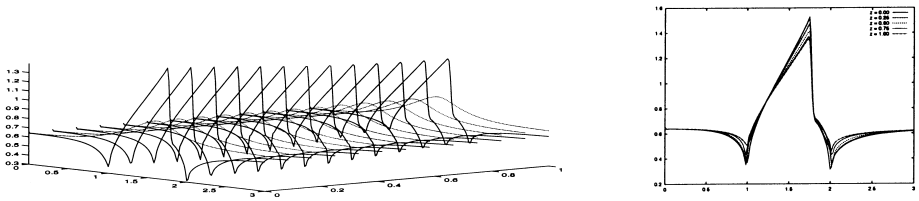

(a) Mach number along the walls

(b) Mach number along the lower wall (projections)

FIGURE 7. Mach number distribution in 3D channel

At the inlet we prescribe the stagnation pressure $p_0(r) = 0.38274$, stagnation density $\rho_0(r) = 1$. The direction of the velocity at the inlet is given by two angles $\alpha_1(r)$ and $\mu_1(r)$.

We use a structured mesh with $90 \times 24 \times 17$ hexahedral cells. Figure 8 shows distribution of the Mach number obtained by the above mentioned modification of 3D Causon's scheme. Figures 9(a)-10(b) show the distribution of the Mach number for different section and on the pressure and suction side of the blade. Similar results were obtained by J. Fořt and J. Halama [7] by using a cell vertex scheme of Ni.

References

[1] Philippe Angot, Jiří Fürst, and Karel Kozel. TVD and ENO schemes for multidimensional steady and unsteady flows. a comparative analysis. In Fayssal Benkhaldoun and Roland Vilsmeier, editors, *Finite Volumes for Complex Applications. Problems and Perspectives*, pages 283–290. Hermes, july 1996.

[2] D. M. Causon. High resolution finite volume schemes and computational aerodynamics. In Josef Ballmann and Rolf Jeltsch, editors, *Nonlinear Hyperbolic Equations - Theory, Computation Methods and Applications*, volume 24 of *Notes on Numerical Fluid Mechanics*, pages 63–74, Braunschweig, March 1989. Vieweg.

[3] Frédéric Coquel and Philippe Le Floch. Convergence of finite difference schemes for conservation laws in several space dimensions: the corrected antidiffusive flux approach. *Mathematics of computation*, 57(195):169–210, july 1991.

[4] Frédéric Coquel and Philippe Le Floch. Convergence of finite difference schemes for conservation laws in several space dimensions: a general theory. *SIAM J. Numer. Anal.*, 30(3):675–700, June 1993.

[5] Vít Dolejší. *Sur des méthodes combinant des volumes finis et des éléments finis pour le calcul d'ecoulements compressibles sur des maillages non structurés.* PhD thesis, L'Université Méditerranée Marseille et Univerzita Karlova Praha, 1998.

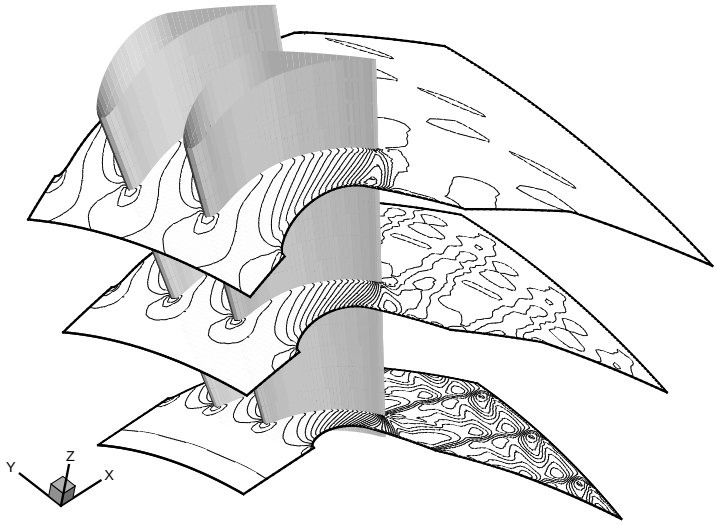

FIGURE 8. Mach number distribution in the 3D turbine.

[6] Miloslav Feistauer, Jiří Felcman, and Mária Lukáčová-Medviďová. Combined finite element-finite volume solution of compressible flow. *Journal of Computational and Applied Mathemetics*, (63):179–199, 1995.

[7] J. Fořt, J. Halama, A. Jirásek, M. Kladrubský, and K. Kozel. Numerical solution of several 2d and 3d internal and external flow problems. In R. Rannacher M. Feistauer and K. Kozel, editors, *Numerical Modelling in Continuum Mechanics*, pages 283–291, September 1997.

[8] Jaroslav Fořt, Miloš Huněk, Karel Kozel, J. Lain, Miroslav Šejna, and Miroslava Vavřincová. Numerical simulation of steady and unsteady flows through plane cascades. In S. M. Deshpande, S. S. Desai, and R. Narasimha, editors, *Fourteenth International Conference on Numerical Methods in Fluid Dynamics*, Lecture Notes in Physics, pages 461–465. Springer, 1994.

[9] Jiří Fürst. Modern difference schemes for solving the system of Euler equations. Diploma thesis, Faculty of Nuclear Science and Physical Engineering, CTU Prague, 1994. (in czech).

[10] Jiří Fürst. *Numerical modeling of the transonic flows using TVD and ENO schemes.* PhD thesis, ČVUT v Praze and l'Universit de la Mditerrane, Marseille, 2000. in preparation.

[11] Jiří Fürst and Karel Kozel. Using TVD and ENO schemes for numerical solution of the multidimensional system of Euler and Navier-Stokes equations. In *Pitman Research Notes*, number 388 in Mathematics Series, 1997. Conference on Navier-Stokes equations, Varenna 1997.

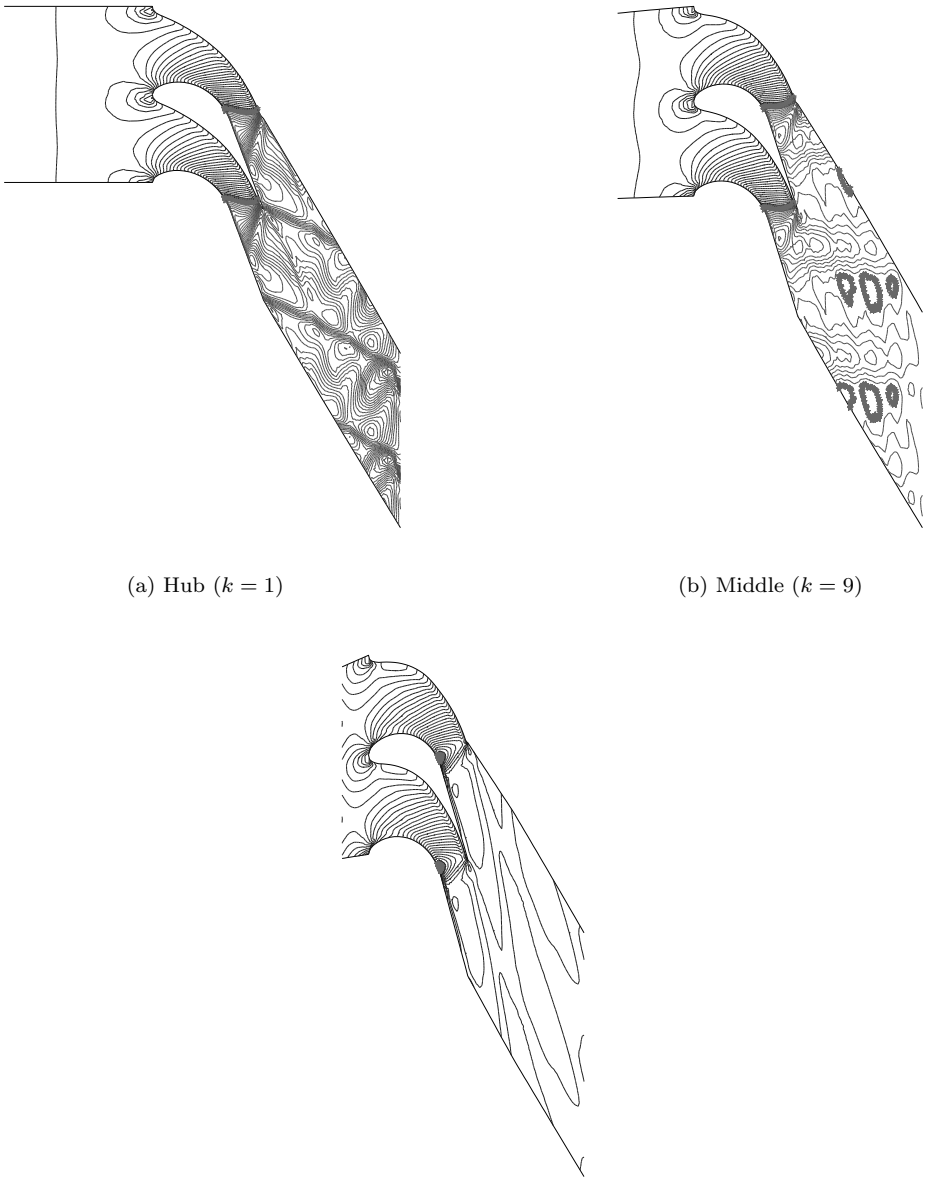

(a) Hub ($k = 1$)

(b) Middle ($k = 9$)

(c) Tip ($k = 18$)

FIGURE 9. Distribution of Mach number for the sections $k = const$.

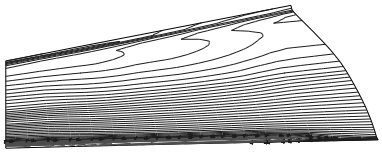

(a) Mach number distribution on the pressure side of the blade

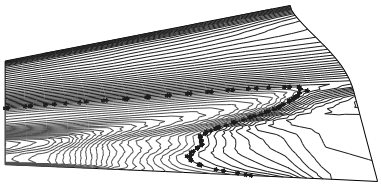

(b) Mach number distribution on the suction side of the blade

FIGURE 10. Distribution of Mach number on the blade

[12] J.B. Goodman and R.J. LeVeque. On the accuracy of stable schemes for 2D scalar conservation laws. *Math. Comp.*, 45:503–520, 1988.

[13] Ami Harten. High resolution schemes for hyperbolic conservation laws. *Journal of Computational Physics*, 49:357–393, 1983.

[14] Michal Janda, Karel Kozel, and Richard Liska. Composite schemes on triangular meshes. In *Proceedings of HYP 2000*, Magdeburg, March 2000. to appear.

[15] Randall J. Le Veque. *Numerical Methods for Conservation Laws*. Birkhäuser Verlag, Basel, 1990.

[16] Stanley Osher and Sukumar Chakravarthy. Upwind schemes and boundary conditions with applications to Euler equations in general geometries. *J. Comp. Phys.*, (50):447–481, 1983.

[17] M. Šťastný and P. Šafařík. Experimental analysis data on the transonic flow past a plane turbine cascade. *ASME Paper*, (91-GT-313), 1990.

Acknowledgment: This work was supported by grants No. 101/98/K001, 201/99/0267 of GAČR and by the Research Plan MSM 98/210000010.

Department of Technical Mathematics,
Faculty of Mechanical Engineering,
Czech Tecnical University,
Karlovo nám. 13
121 35, Praha, Czech Republic
E-mail address: furst@marian.fsik.cvut.cz